Multi-objective design optimization of combined cooling, heating and power system for cruise ship application

Yamin Yan [a], Haoran Zhang [a, b, *], Yin Long [c], Yufei Wang [d], Yongtu Liang [a], Xuan Song [b], James J.Q. Yu [e]

[a] *Beijing Key Laboratory of Urban Oil and Gas Distribution Technology, China University of Petroleum-Beijing, Fuxue Road No. 18, Changping District, Beijing, 102249, China*
[b] *Center for Spatial Information Science, The University of Tokyo, 5-1-5 Kashiwanoha, Kashiwa, Chiba, 277-8563, Japan*
[c] *Department of Environment Systems, Graduate School of Frontier Sciences, The University of Tokyo, 5-1-5 Kashiwanoha, Kashiwa, Chiba, 277-8563, Japan*
[d] *State Key Laboratory of Heavy Oil Processing, China University of Petroleum-Beijing, Fuxue Road No. 18, Changping District, Beijing, 102249, PR China*
[e] *Department of Electrical and Electronic Engineering, The University of Hong Kong, Pokfulam, Hong Kong*

ABSTRACT

In recent years, the size (weight and volume) of cruise ships are experiencing spectacular increase, coherently with the increase in energy consumption and carbon emissions. However, the regulations about pollutant emissions imposed by the International Maritime Organization are becoming more and more strict. In order to face up to this issue, the energy system of cruise ships is constantly being modified. In this paper, the structure of the cruise ship's energy system with multiple facilities such as an internal combustion engine, gas turbine, dual fuel engine, PV panels, and the wind turbine is pre-established. Then, a multi-objective mathematical programming model is formulated to determine the selection and capacity of facilities with minimal total annual cost and size, while the emissions, energy balance and technical constraints are taken into account. By adopting the augmented ε-constraint method, the design and operation strategies could be obtained. As an illustrated example, the model is applied to a real cruise ship, and the Pareto frontier could provide ship designers with well-balanced solutions based on economic and size priorities, and with the increase in the proportion of size objective, the total annual cost increases and size decreases gradually. Compared with the reference energy system, the optimal energy system could reduce the total annual cost by 12.6% if only the economic objective is considered and reduce the size by 21.1% if only the size objective is considered. In multi-objective condition, the CO, NOx, and SOx emissions could be reduced by 29.1%–61.3%, 42.8%–61.3%, and 42.8%–61.3% per year, respectively. Moreover, a sensitivity analysis is conducted, and the result shows that the size and consumption cost of Marine Gas Oil (MGO) and Liquefied Natural Gas (LNG) are more sensitive to the change of the proportion of size objective compared to Heavy fuel oil (HFO) and Marine diesel oil (MDO).

© 2019 Elsevier Ltd. All rights reserved.

1. Introduction

Cruise tourism has become an important niche in the last four decades, since it may provide comfortable service and unique enjoyment with complete amenities and rich entertainment activities. Only 500,000 cruise passengers experienced the sea sail in 1970, while about 30M passengers are expected to take cruises in 2020 with a total economic impact of more than US$ 120B (CLIA, 2016; Perry Hobson, 1993), and global cruising is evolving at a record pace. Cruise tourism has been recognized as the fastest growing segment of the overall global tourism industry, and it has become a major form of tourism in some areas of the world such as the Caribbean, parts of the Mediterranean, and Alaska.

In such a context, the size of cruise ships are also experiencing a spectacular increase from 800 passengers per cruise ship in the 1970s to a projected 6000 passengers in 2020 (Stefanidaki and Lekakou, 2014), accompanied with the increase in energy consumption and carbon emissions. In this scenario, both national and

international energy policies are constantly paying attention to effective strategies and solutions for energy system optimization. Also, International Maritime Organization (IMO), the most noteworthy regulator in the shipping industry, introduced new policy mechanisms and highlighted that the Green House Gases (GHGs) emissions from shipping will be reduced by more than 80% compared to 2010 (Armellini et al., 2018), and the marine energy conservation and emissions reduction are continuously improved. In order to be IMO compliant, some measures are considered to reduce the fuel consumption and carbon emissions (Ancona et al., 2018). Also, other measures are taken into account to improve the operation efficiency of energy system. For instance, Xie (2011) put forward a multi-objective optimization method for preliminary propeller design to improve the efficiency and thrust. In (Motley et al., 2012), the propeller, prime mover (PM) and vessel were regarded as one integrated system, then a brand new and integrated design method was proposed to minimize energy consumption of lifetime and improve the operation efficiency. Nielsen et al. (2018) proposed to optimize engine speed to achieve the goal of improving fuel efficiency.

Several scholars also carried out the discussion on the problem of cruise energy system, consisting of the waste-heat energy recovery estimation of cruise ships (Nguyen and Tenno, 2016), establishment of waste-heat recovery system based on a regenerative organic Rankine cycle (RORC) (Mondejar et al., 2015), modification of the cruise energy system configuration and the utilization of clean fuels (Bicer and Dincer, 2018a). In general, the optimization problem that is related to cruise ship's energy system is solved by establishing appropriate models and applying matching algorithms. Specifically, Tang et al. (2018a) proposed the energy-management model and control method to ensure the safety and effectiveness of the operation. By adopting the adaptive multi-context cooperatively coevolving particle swarm optimization (PSO) algorithm, the globally optimal energy-management is found. Moreover, Tang et al. (2018b) contributed to the operation optimization of hybrid energy system applied in ships. From the viewpoint of economy, the power flow scheduling model is proposed. By adopting the optimal control and model predictive control methods, the power flow dispatch schemes are obtained when the ship is in port. Armellini et al. (2018) proposed a mixed integer nonlinear programming (MINLP) model to analyze the operation efficiency of three possible solutions including the internal combustion engine, internal combustion engine in "eco-friendly" mode with selective catalytic reactor (SCR) and exhaust scrubbers (ES) installed on ship, and gas turbine. Finally, a real cruise ship was set as an example to verify the effectiveness of the model. Ancona et al. (2018) compared the efficiency of standard and hybrid configuration of cruise energy system by establishing the mathematical model with regard to the goals of minimizing fuel consumption and maximizing operation efficiency, and the genetic algorithm was applied to obtain the optimal solution. In summary, the purpose of these studies is to optimize the economic or environmental objectives of the system. Mixed integer linear programming (MILP) and mixed integer nonlinear programming (MINLP) models are the common methods to solve these kind of optimization problems, and the branch-and-bound and heuristic algorithms as well as hybrid method are also widely used to solve the model.

Multi-objective mathematical programming (MOMP) have gained interest for their utility in studying conflicting objectives. In this sense, a number of on-going research works are focusing on the application of MOMP on cruise ships. The main reason is that cruise ships must comply with the new IMO regulations and ship owners also want to ensure their economic benefits. To the best of our knowledge, the first multi-objective paper on maritime shipping was published by Grabowski and Hendrick (1993). The trade-off

between crew size and shipboard safety was discussed. Since then, the trend of applying MOMP to different issues in shipping is becoming more and more obvious. For example, Song and Xu (2012) analyzed the trade-off between carbon emissions and port handling rates. Trivyza et al. (2018) established a MOMP model to optimize economic and environmental benefits of the modern ship energy systems. By using the genetic algorithm NSGA-II, a synthesis decision was made. The result showed that adopting LNG fuel and dual fuel engines technology, as well as introducing other emerging technologies can effectively improve the sustainability of ship energy systems. Furthermore, the trade-off between ship fuel consumption and emissions was elaborated (Hu et al., 2014). Weighting and ε-constraint methods were extensively used to solve the MOMP problem and evolutionary algorithms were also applied to find the Pareto frontier of energy system design and operational strategies between economic and environmental benefits.

Some scholars also proposed the use of hydrogen energy and fuel cells as input energy to meet the energy demands of cruise ships (Bicer and Dincer, 2018b). As hydrogen and fuel cells are very expensive and hydrogen is not readily available everywhere and can be very difficult to control, they began to consider new energy generation technologies applied in the maritime vessels such as wind power (Rodríguez-Rodríguez et al., 2016) and solar photovoltaic (Tang et al., 2018b). However, the research literature on this subject is relatively rare. To the best of our knowledge, there is currently no research to optimize the cruise energy system while considering the fuel consumption cost and facilities' size simultaneously. In this paper, multi-objective mathematical programming (MOMP) model is therefore formulated to obtain the optimized energy dispatch scheme while the emissions, energy balance and technical constraints are taken into account. The first objective is the minimization of total annual cost of cruise ship's energy system, with size as the second objective. By using the augmented ε-constraint method, the Pareto front depicts the best possible trade-off between the economic and size of cruise ship can be obtained. In the end, a real cruise ship is considered as the energy demand side to provide with illustrative case studies.

Overall, this study focus on the several questions entailing: 1) A multi-objective model is proposed to deal with the optimization problem of energy system for cruise ships. 2) An augmented ε-constraint method is presented to solve the problem. 3) The feasibility of the proposed methodology is verified through a real instance. This structure for the remainder of this paper is organized as follows. Section 2 describes the structure of cruise energy system and the problem that needs to be solved. Meanwhile, the framework for solving the problem is also briefly explained. Section 3 gives the details of the methodology and mathematical model as well as the solution method. In Section 4, a detailed description of the case study and the implementation results are provided. Finally, the conclusions of the study are provided in Section 5.

2. Methodology

2.1. Energy system configuration

The principal energy demands of the cruise ships are (i) mechanical demand for propulsion, (ii) electricity for satisfying the hotel loads and auxiliary systems, (iii) thermal energy for space heating, (iv) cooling energy required only in summer. Obviously, the energy system of cruise ship should comply with the IMO regulations, compliant with the safe and reliable operation at a good efficiency level. NOx emissions reduction can be achieved with the after-treatment system, which involves the treatment of exhaust gas with ammonia or urea with a catalyst. With regard to the SOx emissions, sea water scrubbing is a very effective control

method that can achieve a SOx emission level in line with IMO regulation.

Fig. 1 gives the overall structure of the cruise ship's energy system. There are three options for propulsion system. The first and typical one is internal combustion engine (ICE) with the exhaust gas treatment facilities (SCR and ES) must be installed to meet the IMO emission standards for NOx and SOx, and the exhaust gas after treatment is discharged to the atmosphere. Another alternative option is the installation of gas turbines (GT) which operate on MGO to produce the mechanical and thermal energy. The last option is the installation of Dual fuel (DF) engines which operate with LNG fuels or Marine Diesel Oil (MDO) (Livanos et al., 2014), and LNG infrastructure has been developed in the last few years (Burel et al., 2013). In order to improve the efficiency and flexibility of the system, exhaust gas boilers (EGB) are considered to be installed in the energy system. The non-propulsive electric loads could be satisfied by the engines and additionally wind turbines (WT) as well as PV panels (PV). The waste gas from the ICE, GT and DF engines is absorbed by the EGB to produce heat to meet the thermal demand of cruise ship. The cooling system for hotel service is realized by compression chillers (COC).

2.2. Problem description

In this paper, we proposed an optimization framework that enables ship owners to obtain the design and operation strategies of energy system with minimal total annual cost and size, as shown in Fig. 2, in which the framework can be divided into four steps: (1) pre-processing inputs, (2) determination of case studies, (3) model establishment, (4) result and analysis. In the first step, the input parameters should be pre-defined, which include energy demands, weather information of a track, cost and technical information as well as size of facilities. In the second step, four cases are considered to compare the calculation results, which will be described in section 4.1.5. In the modeling step, based on the preferences of different ship designers, the design and operation strategies of energy system for cruise ships are obtained with minimal total annual cost and size, while considering the emission, energy balance, and technical constraints. In particular, when only one objective is considered, the model can be formulated as MILP, and when both two objectives are considered, the model can be formulated as MOMP. Finally, the solutions obtained under the single-objective and multi-objective optimization are compared with the reference energy system from the perspectives of the economy, environment, and size.

3. Mathematical model

3.1. Multi-objective model

Establishing a MOMP model is a typical way to solve the problem mentioned in section 2.2. We take the total cost and size as the objectives. In order to obtain the design and operation strategies of the energy system for cruise ships, the emission, energy balance and technical constraints are considered. In accordance with the augmented ε-constraint method, the final optimization results can be obtained. To describe the method presented in this paper and facilitate understanding by readers, the model can be depicted by the following mathematical form:

$$\min\{f_1(d_1, o_1, p_1), f_2(d_2, o_2, p_2)\}$$
$$\text{s.t. } \varphi(d, o, p) = 0 \tag{1}$$
$$\psi(d, o, p) \leq 0$$

where d represents the decision variable for the selection and sizing of the facilities, $d = \{d_1, d_2\}$, o represents the decision variable of the energy system operation, $o = \{o_1, o_2\}$, p defines the input parameters of the model, $p = \{p_1, p_2\}$, f represents the objective function related to d and o, φ and ψ represent the equality and inequality constraints respectively.

In this study, single-objective optimization is also taken into account, and the problem can be formulated as a MILP model, and the model can be performed using the following compact form:

$$\min\{f_1(d_1, o_1, p_1)\}$$
$$\text{s.t. } \varphi(d_1, o_1, p_1) = 0 \tag{2}$$
$$\psi(d_1, o_1, p_1) \leq 0$$

$$\min\{f_2(d_2, o_2, p_2)\}$$
$$\text{s.t. } \varphi(d_2, o_2, p_2) = 0 \tag{3}$$
$$\psi(d_2, o_2, p_2) \leq 0$$

3.2. Decision variables

There are two types of decision variables consisting of continuous and integer ones. The continuous variables describe the selection and capacity of facilities, energy consumption, as well as the
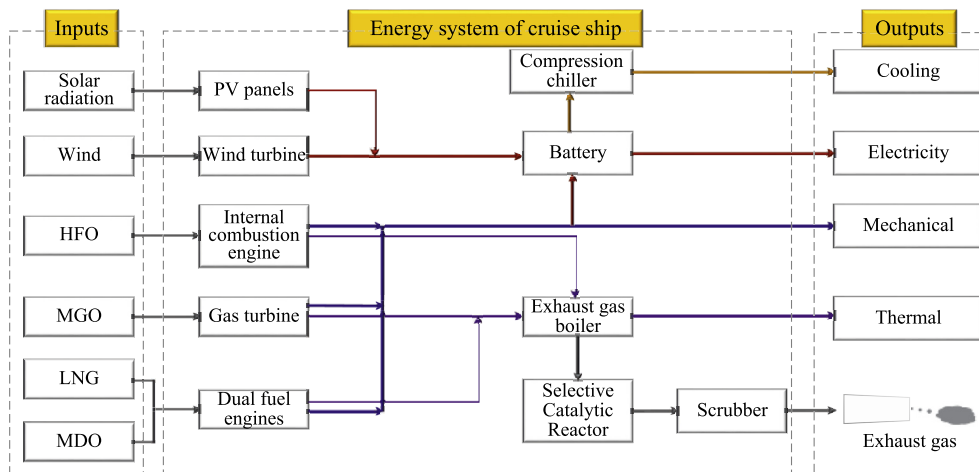

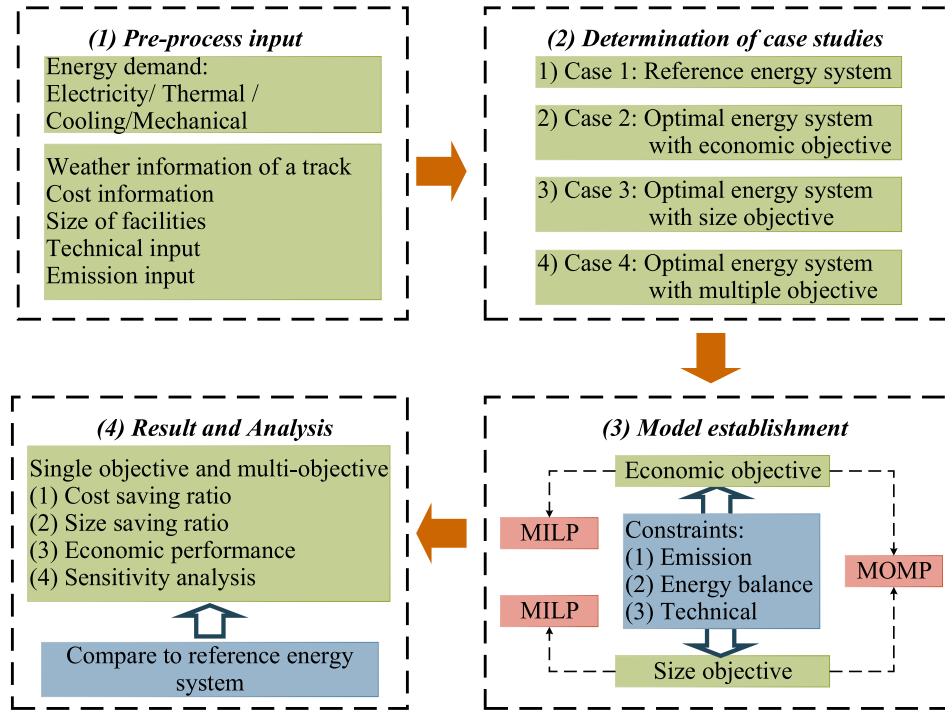**Fig. 1.** Structure of the cruise ship's energy system.

Fig. 2. Technical roadmap of the proposed optimization framework.

input and output energy flows of the cruise ship's energy system. The integer variables describe whether the facility is selected to be installed in the cruise ship or not.

3.3. Objective function

Two objectives are considered in this study, including the economic and size ones.

(1) Economic objective

The economic objective of this model is defined as shown in Eq. (4), which indicates the total annual cost of the cruise ship's energy system. In detail, f_1 is the investment cost of all facilities as formulated in Eq. (5), which is composed of fixed cost and linear-capacity cost. f_2 defines the annual cost of energy consumption as formulated in Eq. (6). Moreover, the annual investment cost of facility i is calculated by the capital recovery factor CRF_i, which is formulated in Eq. (7).

$$f_{\cos t} = f_1 + f_2 \tag{4}$$

$$f_1 = \sum_{i \in I} (B_i C_{FCi} + V_i C_{LCi}) CRF_i \tag{5}$$

$$f_2 = \sum_{s \in S} \sum_{ts \in TS_s} \sum_{m \in M} EX_{s,ts,m} P_m w_{s,ts} \tag{6}$$

$$CRF_i = \frac{r(r+1)^{lifetime_i}}{(r+1)^{lifetime_i} - 1} \tag{7}$$

where, the binary variable B_i defines the installation of facility i in a cruise ship, V_i is a continuous variable representing the capacity of facility i [kW for conversion facilities, kWh for battery, m^2 for PV panels and wind turbines]. C_{FCi} is the fixed cost of facility i [€], C_{LCi}

is the linear-capacity cost of facility i [€/(kW, kWh, m^2)], CRF_i defines the capital recovery factor of facility i, $lifetime_i$ is the lifetime of facility i and r is the discount rate, $EX_{s,t,m}$ is the energy consumption of energy carrier m at time step ts for operation state s [kWh], P_m is the price of energy carrier m [€/kWh], $w_{s,ts}$ is the total number of time step ts for operation state s.

(2) Size objective

The size objective of this model is defined as shown in Eq. (8). To be specific, f_{space} indicates the total occupied space of energy system as formulated in Eq. (9), which is composed of all facilities and energy carriers. Similarly, f_{weight} defines the total weight of energy system as formulated in Eq. (10).

$$f_{scale} = \alpha f_{space} + f_{weight} \tag{8}$$

$$f_{space} = \varepsilon V_{PV} + \phi V_{WT} + \sum_{i \in I} V_i S_{LSi} + \sum_{s \in S} \sum_{ts \in TS_s} \sum_{m \in M} EX_{s,ts,m} S_{LOm} \tag{9}$$

$$f_{weight} = \lambda V_{PV} + \beta V_{WT} + \sum_{i \in I} V_i W_{LSi} + \sum_{s \in S} \sum_{ts \in TS_s} \sum_{m \in M} EX_{s,ts,m} W_{LOm} \tag{10}$$

where, f_{space} and f_{weight} are the total occupied space and weight of facilities and energy carriers, the constant α is a scaling factor, so that f_{space} and f_{weight} could have the same order of magnitude, S_{LSi} defines the linear-capacity occupied space of facility i [m^3/(kW, kWh)], and W_{LSi} defines the linear-capacity and weight of facility i [kg/(kW, kWh)], S_{LOm} defines the linear-consumption occupy space of energy carrier m [m^3/kWh], and W_{LOm} defines the linear-consumption weight of energy carrier m [kg/kWh]. Besides, ε and ϕ are parameters representing the height of PV panels and wind turbine [m], λ and β are two conversion parameters [kg/m^2].

3.4. Emission constraints

In order to comply with the IMO regulations, the emission constraints are necessary, including the carbon emissions, NOx emissions and SOx emissions.

$$\sum_{ts \in TS_s} \sum_{m \in M} EX_{s,ts,m} C_{s,m} w_{s,ts} \leq Carbon_s \quad \forall s \in S \tag{11}$$

$$\sum_{ts \in TS_s} \sum_{m \in M} EX_{s,ts,m} N_{s,m} w_{s,ts} \leq Nitrogen_s \quad \forall s \in S \tag{12}$$

$$\sum_{ts \in TS_s} \sum_{m \in M} EX_{s,ts,m} Su_{s,m} w_{s,ts} \leq Sulfur_s \quad \forall s \in S \tag{13}$$

In these equations, $C_{s,m}$ represents the carbon emission factor of energy carrier m for operation state s, $Carbon_s$ indicates the carbon emission limit of operation state s, $N_{s,m}$ represents the NOx emission factor of energy carrier m for operation state S, $Nitrogen_s$ indicates the NOx emission limit of operation state s, $Su_{s,m}$ represents the SOx emission factor of energy carrier m for operation state S, $Sulfur_s$ indicates the SOx emission limit of operation state s.

3.5. Energy balance constraints

To satisfy the energy demand of cruise ship, mechanical, electricity, thermal and cooling energy balances constraints are described as follows.

The mechanical demand for propulsion has to be satisfied by the total electricity provided by ICE, GT, and DF.

$$n_{ICE,ele}Q_{s,ts,ICE} + n_{GT,ele}Q_{s,ts,GT} + n_{DF,ele}Q_{s,ts,DF} - Q_{s,ts,bat}$$
$$= MD_{s,ts} \quad \forall s \in S, \forall ts \in TS_s \tag{14}$$

where, $n_{ICE,ele}$ represents the efficiency of ICE conversion to electricity, $Q_{s,ts,i}$ is a continuous variable indicating the energy input to the facility i at time step ts for operation state s, $MD_{s,ts}$ is the mechanical demand of cruise ship at time step ts for operation state s.

For electricity, the sum of electricity demand has to be met by the electricity provided by PV panels and wind turbines as well as the engines (ICE, GT, and DF).

$$n_{WT}V_{WT}IN_{s,ts}^{WT} + n_{PV}V_{PV}IN_{s,ts}^{PV} + Q_{s,ts,bat} - Q_{s,ts,COC} + ES_{s,ts}^{dis} - ES_{s,ts}^{ch}$$
$$= ED_{s,ts} \quad \forall s \in S, \forall ts \in TS_s \tag{15}$$

where, n_i defines the operation efficiency of the facility i, $IN_{s,ts}^{PV}$ and $IN_{s,ts}^{WT}$ are the incoming solar radiation and wind power at time step ts for operation state s, respectively, $ES_{s,ts}^{dis}$ and $ES_{s,ts}^{ch}$ are the discharging and charging rate of the battery, respectively, $ED_{s,ts}$ is the electricity demand of cruise ship at time step ts for operation state s.

The waste gas from the ICE, GT and DF engines is absorbed by the exhaust gas boiler to produce secondary heat to meet the thermal demand of cruise ship, and excess exhaust gas is discharged to the atmosphere after being treated to the standard. Meanwhile, the cooling demand is meet by compression chiller, and excess cooling energy is not stored.

$$(n_{ICE,th}Q_{s,ts,ICE} + n_{DF,th}Q_{s,ts,DF} + n_{GT,th}Q_{s,ts,GT})n_{EGB} - Q_{s,ts,SCR}$$
$$= TD_{s,ts} \quad \forall s \in S, \forall ts \in TS_s \tag{16}$$

$$n_{COC}Q_{s,ts,COC} \geq CD_{s,ts} \quad \forall s \in S, \forall ts \in TS_s \tag{17}$$

where, $TD_{s,ts}$ is the thermal demand of cruise ship at time step ts for operation state s, $CD_{s,ts}$ is the cooling demand of cruise ship at time step ts for operation state s.

The following equation constraints are required to ensure the energy input to the facilities. It's necessary to indicate that the DF engine has two operation modes: one is gas modes, in which the fuel is gas, the other is diesel mode, and the diesel is the fuel.

$$Q_{s,ts,ICE} = EX_{s,ts,HFO} \quad \forall s \in S, \forall ts \in TS_s \tag{18}$$

$$Q_{s,ts,GT} = EX_{s,ts,MGO} \quad \forall s \in S, \forall ts \in TS_s \tag{19}$$

$$\begin{cases} Q_{s,ts,DF_{gas}} = EX_{s,ts,LNG} \\ Q_{s,ts,DF_{diesel}} = EX_{s,ts,MDO} \end{cases} \quad \forall s \in S, \forall ts \in TS_s \tag{20}$$

$$n_{ICE,th}Q_{s,ts,ICE} + n_{DF,th}Q_{s,ts,DF} + n_{GT,th}Q_{s,ts,GT}$$
$$= Q_{s,ts,EGB} \quad \forall s \in S, \forall ts \in TS_s \tag{21}$$

$$Q_{s,ts,ICE}n_{ICE}n_{EGB} \geq Q_{s,ts,SCR} \quad \forall s \in S, \forall ts \in TS_s \tag{22}$$

$$n_{SCR}Q_{s,ts,SCR} = Q_{s,ts,ES} \quad \forall s \in S, \forall ts \in TS_s \tag{23}$$

The role of the battery is to deal with periodic fluctuations, and the electricity stored in the battery is related to the charging and discharging electricity flows as well as electricity losses. In an operation period, Eq. (24) can be applied to any operation state other than the first operation state. Conversely, Eq. (25) can only be applied to the first operation state. It's necessary to point out that the electricity stored in the battery during the first hour of the first operating state should be equal to the electricity stored in the last hour of the last operating state.

$$S_{s,1} = n^{loss}S_{s,tm_{s-1}} + n^{ch}ES_{s,1}^{ch} - ES_{s,1}^{dis}/n^{dis} \quad \forall s \in S, \forall ts \in TS_s \backslash \overline{TS_s} \tag{24}$$

$$S_{1,1} = n^{loss}S_{s,tm_s} + n^{ch}ES_{s,1}^{ch} - ES_{s,1}^{dis}/n^{dis} \quad \forall s \in S, \forall ts \in \overline{TS_s} \tag{25}$$

where, $S_{s,ts}$ is a continuous variable that defines the amount of electricity stored during time ts for operation state s, $S_{s,1}$ represents the electricity stored in the battery in the first hour of the operating state s, S_{s,tm_s} represents the electricity stored in the battery in the last hour tm_S of the operating state s, n^{loss}, n^{ch}, and n^{dis} represent the electricity losses, electricity charging and discharging efficiencies, respectively.

3.6. Technical constraints

To link the fixed investment cost C_{LCi} to the selection of a facility i in the objective function, the following constraint is necessary, in which Max is the upper limit of capacity and Min is a small number to restrict the capacity of facility to greater than 0 once the facility is selected. Here, Min is set as 0.2.

$$B_iMin \leq V_i \leq B_iMax \quad \forall i \in I \tag{26}$$

In addition, the operating power of the energy generation and battery cannot exceed the rated capacity.

$$n_j Q_{s,ts,j} \leq V_j \ \forall s \in S, \ \forall ts \in TS_s, \ \forall j \in J \tag{27}$$

$$S_{s,ts} \leq V_{ES} \ \forall s \in S, \ \forall ts \in TS_s \tag{28}$$

There is an upper limit in the total capacities of PV panel and wind turbine due to the limited installation space of cruise ships.

$$V_{PV} \leq S_{\max}^{PV} \tag{29}$$

$$V_{WT} \leq S_{\max}^{WT} \tag{30}$$

It's worthy to note that SCR and ES must be used to reach the regulation of NOx emissions if HFO is used as the PM. Meanwhile, the EGB must be used to

$$B_{ICE} = B_{SCR} \tag{31}$$

$$B_{SCR} = B_{ES} \tag{32}$$

3.7. Optimization method

As mentioned earlier, the study has two objective functions that need to be minimized: the first objective is to minimize the total annual cost, and the second objective is to minimize the size of cruise ship's energy system. Generally, the weighting method and ε-constraint method are most widely applied to solve MOMP problem. They can provide a representative subset of the Pareto set, which is sufficient in most cases. For example, Li et al. (2016) established a MOMP model with minimal total annual cost and carbon emissions and the optimal design. Operation strategies of distributed energy system are obtained by using the weighting method. Di Somma et al. (2017) introduced weighting method to consider both the total cost and primary exergy input. Also, ε-constraint method was adopted (Xing et al., 2019) to deal with the natural gas allocation strategy between industrial parks under gas shortage. However, the augmented ε-constraint method can find the optimal solutions more quickly and effectively than the weighting method when solving the multi-objective mathematical programming (MOMP) problem (Esmaili et al., 2011), and the number of solutions can be controlled by appropriately adjusting the range of each objective function (Mavrotas, 2009). Therefore, the augmented ε-constraint method is chosen to solve the MOMP problem in this paper, which can be expressed as follows:

In the ε-constraint method, one of the objective functions is used as the main objective function, and the other objective functions are added as constraints to the feasible solution space for optimization as presented in Eq. (33). However, the effectiveness of the general ε-constraint method solution cannot be guaranteed, which means that an inefficient solution may be produced. Based on the analysis above, the augmented ε-constraint method is used to overcome the drawback in this paper. Firstly, the inequality constraints of the objective function in Eq. (33) is transformed into equality constraints by introducing slack variables (Esmaili et al., 2011). Then, the main objective function is augmented by the sum of the slack variables. Therefore, the augmented ε-constraint method can be expressed as Eq. (34):

$$\text{Minimize} \ \ f_1(x) \ \text{Subject to} \ f_2(x) \leq e_2, f_3(x) \leq e_3, \cdots, f_p(x)$$
$$\leq e_p \ \ x \in S$$
$$\tag{33}$$

$$\text{Minimize} \ (f_1(x) - eps \times (s_2 + s_3 + \cdots + s_p)) \ \text{Subject to} \ f_2(x) + s_2$$
$$= e_2, f_3(x) + s_3 = e_3, \cdots, f_p(x) + s_p = e_p \ \ x \in S \ and \ s_i \in R^+.$$
$$\tag{34}$$

where, *eps* is a small number usually between 10^{-3} and 10^{-6} (Mavrotas, 2009).

4. Case study

The optimization model was applied to a cruise ship operating in the Baltic Sea between Stockholm and Mariehamn. The cruise ship is built in 2004 and is 176.9 m long and 28.6 m wide with a design speed equal to 21 knots. It can accommodate up to 1,800 passengers and is equipped with restaurants, nightclubs and bars, as well as saunas and pools. The ship departs from Stockholm at around 6:00 p.m. until it reaches the open sea and stops there for a night before arriving at Mariehamn in the early morning. Then the ship leaves Mariehamn at around 9:00 a.m. and arrived at Stockholm around 4:00 p.m., and it travels the same route every day of the whole year just as shown in Fig. 3. Based on this, the ship's operation state can be divided into three types (Ancona et al., 2018): (i) navigation, (ii) port stay and sea stay, (iii) maneuvering, which accounts for 59%, 33%, and 8% of the operation period, respectively.

4.1. Input data

4.1.1. Energy demand

The principal energy demands of the cruise ship is presented in Fig. 4 (Ancona et al., 2018), including the mechanical, electricity, thermal and cooling energy. Here, three typical days are selected to represent winter, summer, and mid-season with a duration of 182, 62 and 121 days, respectively.

It can be easily found that the mechanical energy demand is the same on three typical days. There is no mechanical energy requirement when the cruise ship is at the state of port stay or sea stay, while the electricity and thermal energy as well as cooling energy are needed to ensure the boarding and landing services (port stay) of the passengers and their comfort on board (sea stay). As the cruise ship leaves the port, the demand for mechanical energy starts to increase and then decreases as it enters the port, reaching the maximum during the state of navigation. Different from the mechanical demand, the demands for electricity and thermal energy are always required and less affected by the cruise ship's operation states, which can be explained by the need to ensure the passengers' comfort services and the operation of related equipment. The demand for thermal energy is high in summer, but it shows the opposite trend in winter. The cooling energy is only required in summer.

4.1.2. Solar radiation and wind power

Solar radiation and wind power are representative weather information that input into the model. The Baltic Sea is located in the transition zone between temperate maritime climate and continental climate, and the west wind dominates the whole year. Since the north Atlantic drift is difficult to enter the Baltic sea, the temperature is relatively low in winter and not high in summer. Taking the climate information above into account, together with a data collection (Finnish Meteorological Institute), allows to estimate the solar radiation intensity of the Baltic Sea on three typical days, as shown in Fig. 5. The wind power density is mainly related to two factors: wind speed and air density. Specifically, the wind energy density is proportional to the cube of the wind speed and is also
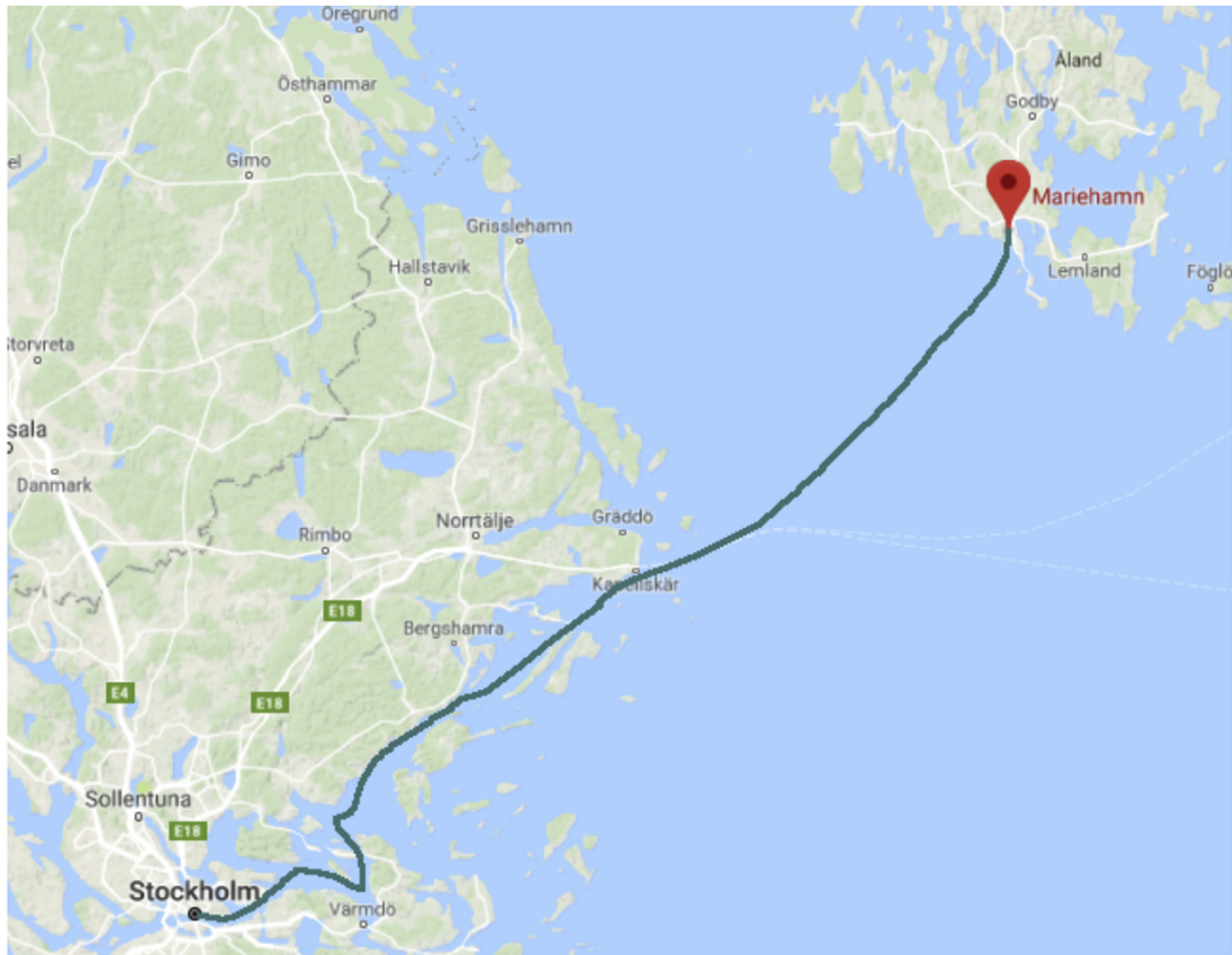
Fig. 3. Route of the cruise ship.

proportional to the air density. Moreover, the air density in winter is higher than that in summer. Fig. 6 presents the wind speed and wind power density in the Baltic Sea (Finnish Meteorological Institute). It can be seen that the wind speed is high in winter and low in summer. Based on the analysis above, the low air density and low wind speed in summer lead to low wind power density, thereby generating less electricity.

4.1.3. Price and emission factors of energy carriers

The prices of primary energy carriers consisting of HFO, MGO, LNG, and MDO are collected in (Burel et al., 2013). In detail, the unit price of HFO is 0.0454 €/kWh, and the unit prices of MGO, LNG, and MDO are set as 0.0782 €/kWh, 0.0156 €/kWh, and 0.0692 €/kWh, respectively. Meanwhile, Table 1 shows the pollutant emission factors of primary energy carriers, including the CO, CO_2, NOx, and SOx. It's necessary to indicate that the concentration of pollutants can reach 100 mg/m^3 after the exhaust gas from ICE is treated by SCR and ES, which means that the emissions of NOx and SOx can be significantly reduced by the treatment system. Moreover, this level of emissions can meet even more strict limitations in the future.

4.1.4. Technical and cost information of facilities

Table 2 gives the technical and economic information of facilities, which includes the fixed cost (Armellini et al., 2018), linear capacity-dependent cost (Burel et al., 2013; Chen et al., 2018), efficiency (Di Somma et al., 2017; Mavromatidis et al., 2018), and

lifetime (Yang et al., 2017). Among the three propulsion engines, it can be noted that DF engine has the highest mechanical energy generation efficiency and the most expensive cost. Moreover, the upper bounds of installed capacity for PV panels and wind turbines are described in Eq. (29) and Eq. (30). In addition, the size of engines and energy carriers are summarized in Table 3 (Livanos et al., 2014).

4.1.5. Determination of case studies

In order to compare the calculation results of single objective and multi-objective, four cases are considered in this section:

(1) In the first case, a reference energy system is adopted, in which the mechanical and electricity as well as heating demands are satisfied by ICE and COC provides cooling energy to passengers on the cruise ship. Note that only economic objective is taken into account.
(2) In the second case, the proposed optimization energy system is adopted and only economic objective is taken into account.
(3) In the third case, the proposed optimization energy system is adopted and only size objective is considered.
(4) In the fourth case, the proposed optimization energy system is adopted, and economic and size objectives are both put into consideration.

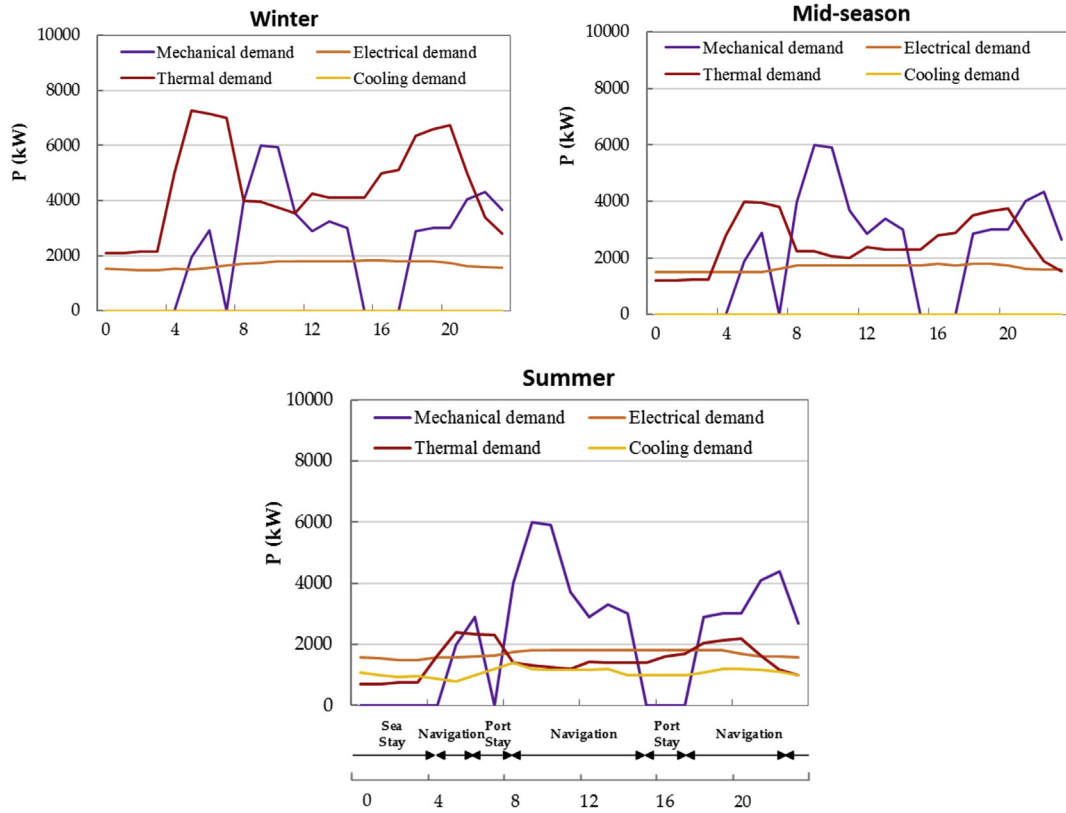The first three cases can be formulated as a MILP. Based on the

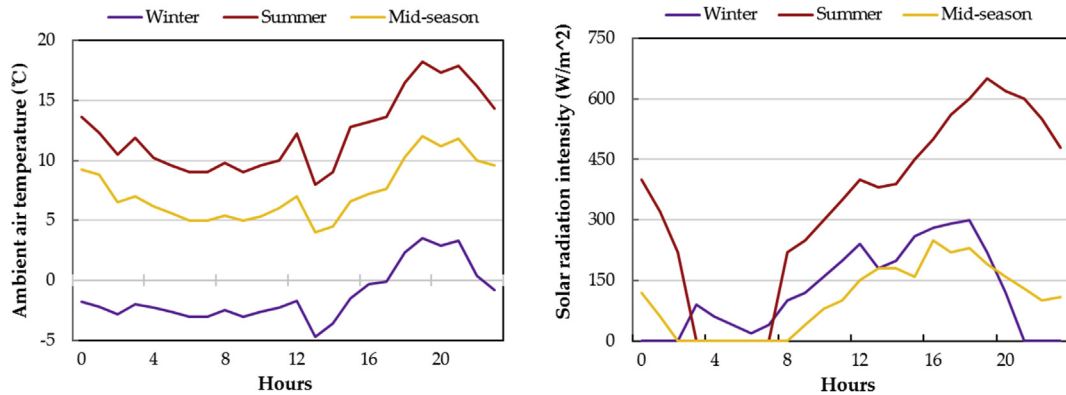**Fig. 4.** Energy demands for the cruise ship on three typical days.

Fig. 5. Ambient air temperature and solar radiation intensity of the Baltic Sea on three typical days.

computer with 4 GB of RAM memory and the Intel Xeon E5-2630v3 (2.4 GHz) dual thread parallel processor, the model was programmed with MATLAB R2015a, and solved by GUROBI 8.1.0 to calculate the global optimum. The last case is formulated as a MOMP problem, and the augmented ε-constraint method is adopted. After calculation, the optimization problem can be solved within a few seconds, and the results will be discussed in the next section.

4.2. Results

4.2.1. Optimization of the reference energy system

Fig. 7 shows the optimal configuration of the cruise ship's energy system under case 1. It is not difficult to predict that the total capacity of compression chillers is strongly related to the maximal

cooling demand of 1400 kW. Also, ICE is operated to provide the heating and electricity as well as mechanical energy, which can be found in Fig. 8. The role of battery is to cope with cyclical fluctuations, and its capacity reaches a maximum of 5000 kWh, which means that the battery is committed to achieving the economic goal by reducing total electricity input while meeting the electricity demand of cruise ship. The selective catalytic reactor with a capacity of 3133 kW and exhaust scrubber with a capacity of 2506 kW are installed for the system to be IMO compliant. Moreover, Fig. 9 gives the energy consumption of the reference energy system. To be specific, the total annual HFO consumption is equal to 127.02 GWh, and the total cost is equal to 7,531,502 €. Meanwhile, the annual carbon emissions, NOx emissions, and SOx emissions can be calculated as 80.8 t, 950.3 t, 589.9 t, respectively.
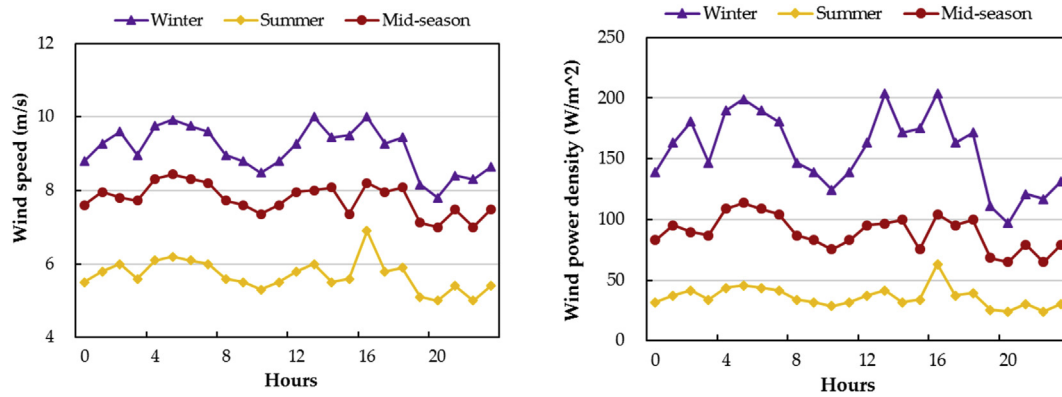
Fig. 6. Wind speed and wind power density of the Baltic Sea on three typical days.

Table 1
Emissions factor for energy carriers (Ancona et al., 2018; Armellini et al., 2018; Burel et al., 2013).

Emission factor (kg/kg fuel)	HFO	HFO_SCR	MGO	LNG	MDO
CO	0.0074	<0.0001	0.0022	-	0.0028
CO_2	3.2060	<0.0001	3.2060	2.75	3.2060
NOx	0.0870	<0.0001	0.0080	-	0.0873
SOx	0.0540	<0.0001	0.0020	-	0.0026

4.2.2. Optimization of the energy system with economic objective

In this section, the proposed optimization energy system is adopted, and only the economic objective is taken into account. Fig. 10 shows the optimal configuration of the energy system under case 2. Notably, PV panels and wind turbines are not selected as the energy provider because of the low energy input. This emphasizes the limitations of using renewable energy on cruise ships, namely the potential of PV panels and wind turbines can be better exploited only when the input energy is sufficiently high. The total capacity of the battery reaches the capacity limit of 5,000 kWh, and the total capacity of the compression chiller is strongly related to the maximal cooling demand, as no cooling storage is considered to be installed on the cruise ship considering the cooling demand is only needed in summer. Moreover, the total capacity of internal combustion engines is the largest among all the facilities, mostly due to the low investment cost and high efficiency. Interestingly, the internal combustion engines do not provide the most energy which can be found in Fig. 11(a) and (b). On the contrary, the dual fuel engines supply the most mechanical and electricity as well as thermal energy to the cruise ship, thus consuming more LNG. This shows that LNG is more likely to achieve economic objective because of low energy price. Meanwhile, Fig. 12 gives the energy consumption of optimized energy system, which further illustrates the superiority of LNG.

Table 2
Technical and cost information of facility.

Facility	Fixed cost (€)	Linear capacity-dependent cost (€/kW, €/kWh, €/m²)	Rated efficiency		Lifetime (a)
			Electrical	Thermal	
PV panels	5,013	2,100	17%	-	25
Wind turbine	2,600	1,262	35%	-	25
Compression chiller	43,235	131	-	COP = 4.7	25
Internal combustion engine	206,862	689	40%	26%	15
Gas turbine	259,783	764	32%	26%	15
Dual fuel engine	299,150	1,362	47%	21%	15
Exhaust gas boiler	57,627	174	-	88%	15
Selective catalytic reactor	3,546	154	-	-	15
Exhaust scrubbers	2,386	110	-	-	15
Batteries	1685	12.5	90%	-	20

Table 3
Size of facilities and energy carriers.

Facility	Linear capacity-dependent volume (10^{-3} m³/kW, 10^{-3} m³/kWh)	Linear capacity-dependent weight (kg/kW, kg/kWh)
Compression chiller	13.0	4.3
Internal combustion engine	42.3	14.5
Gas turbine	24.1	8.0
Dual fuel engine	28.6	17.9
Exhaust gas boiler	8.9	1.8
Selective catalytic reactor	13.1	4.6
Exhaust scrubbers	11.2	5.0
Batteries	1.3	1.2
HFO	12.503	0.086
MGO	12.182	0.098
LNG	33.470	0.072
MDO	12.344	0.091

Fig. 7. Optimal configuration of the cruise ship's energy system under case 1.

Fig. 9. Energy consumption of the cruise ship's energy system under case 1.

(a)

Fig. 10. Optimal configuration of the cruise ship's energy system under case 2.

4.2.3. Optimization of the energy system with size objective

In this section, the proposed optimization energy system is adopted, and only the size objective is considered. Fig. 13 shows the optimal configuration of the energy system under case 3. Similarly, PV panels and wind turbines are not selected, which further illustrates that they don't have advantages in economy or size. It is noteworthy that the total capacity of gas turbines is the largest among all the facilities, which shows the superiority for the size objective. This result can be attributed to the low size of facility and prime mover MGO. Besides, it can be found that internal combustion engines rank second in installed capacity, due to the low size of prime mover HFO. Above all, the energy generated by the cooperation between the internal combustion engines and the gas turbines is more in line with the electricity and thermal energy requirements of the cruise ship, which can be found in Fig. 14. In detail, internal combustion engines meet most of the mechanical, electrical as well as thermal requirements of the cruise ship in winter, and gas turbines provide most of the energy to cruise ship in mid-season.

Fig. 15 shows the energy consumption of the cruise ship's energy system in three seasons. To be specific, HFO in winter, MGO in summer and autumn as the prime mover to meet the energy demands of the cruise ship. Moreover, the total size of the optimal energy system is calculated as 289,124 (including the weight of 283 ton and the occupied space of 6,532 m³), and the annual carbon emissions, NOx emissions, and SOx emissions are 57.3 t, 543.2 t, 315.4 t, respectively. Compared with the reference energy system, the total size is reduced by 21.1%, and the carbon emissions, NOx emissions, and SOx emissions are reduced by 29.1%, 42.8%, 46.5%

(b)

Fig. 8. Operation strategies of the optimized energy system on three typical days under case 1 for (a) mechanical and electricity; (b) thermal energy.

Furthermore, the total annual cost of the optimal energy system under case 2 is calculated as 6,581,777 €, and the annual carbon emissions, NOx emissions, and SOx emissions are 31.2 t, 367.9 t, 227.8 t, respectively. Compared with the reference energy system, the total annual cost is reduced by 12.6%, and the carbon emissions, NOx emissions, and SOx emissions are reduced by 61.3%, 61.3%, 61.3% per year, respectively.
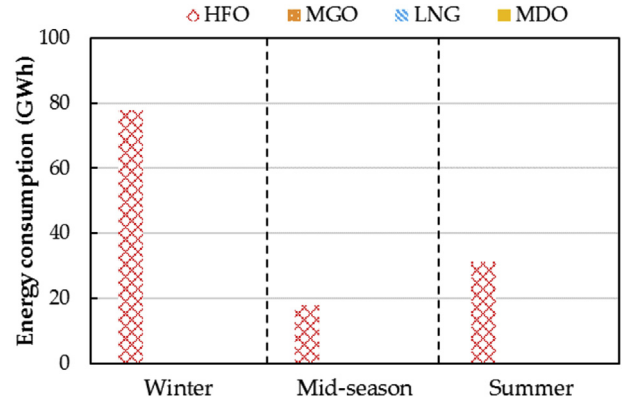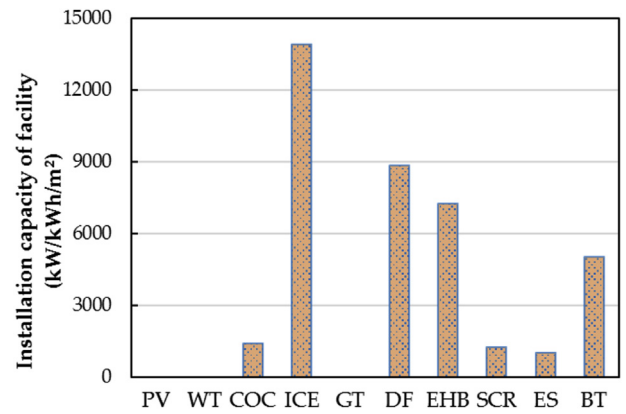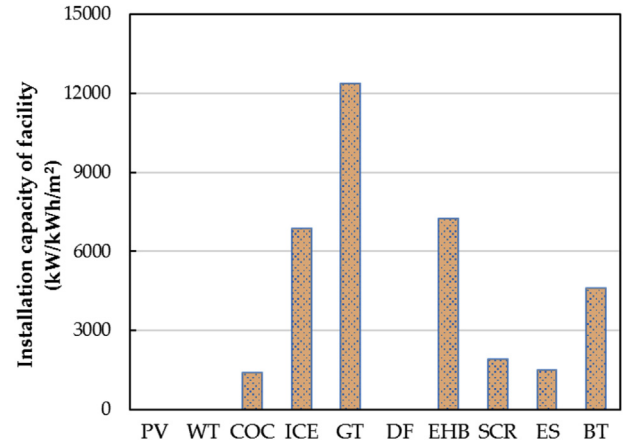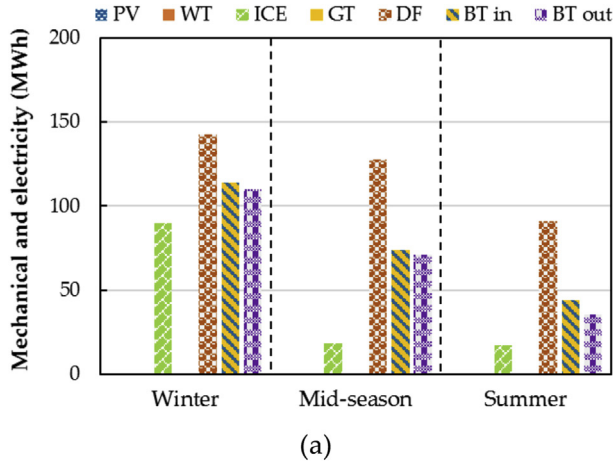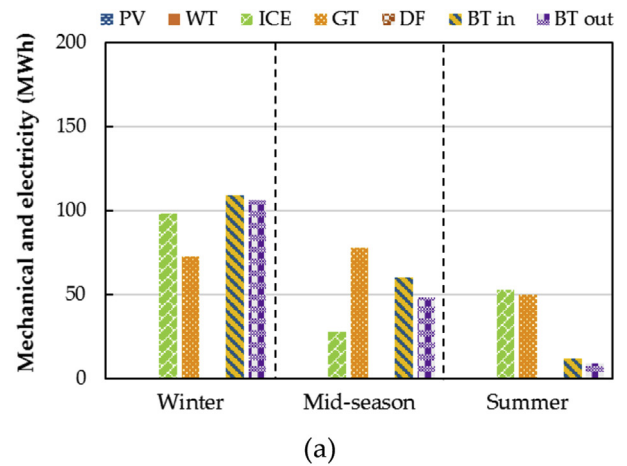
(a)

(b)

Fig. 11. Operation strategies of the optimized energy system on three typical days under case 2 for (a) mechanical and electricity; (b) thermal energy.

Fig. 12. Energy consumption of the cruise ship's energy system under case 2.

Fig. 13. Optimal configuration of the cruise ship's energy system under case 3.
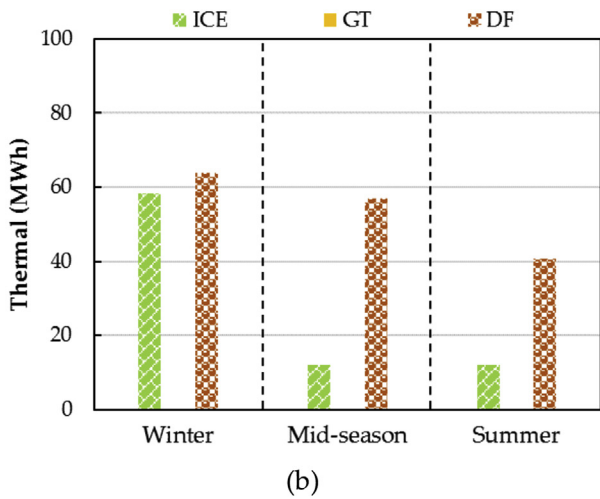

(a)

(b)

Fig. 14. Operation strategies of the optimized energy system on three typical days under case 3 for (a) mechanical and electricity; (b) thermal energy.
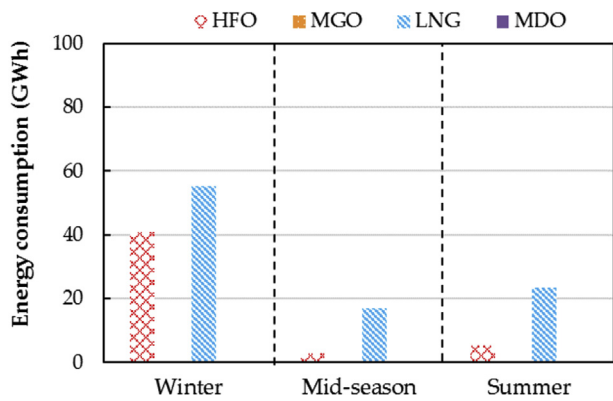
per year, respectively. However, the total annual cost is equal to 10,747,140 € and the cost saving ratio is equal to a negative value of −42.7%, indicating that the economic performance is poor when only the size objective is considered.

4.2.4. Optimization of the energy system with multiple objectives

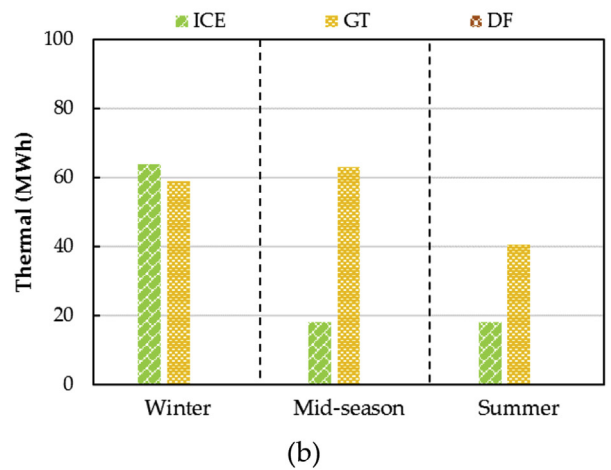In addition to economic objective, size is also an important factor in designing the energy system of cruise ships. Therefore, the optimization of the energy system is performed by considering both economic and size objectives in this section. Fig. 16 shows the Pareto frontier. Point a is obtained under the economic objective and point e is obtained under the size objective, which have been discussed in previous section. The points between these two extreme points are found by subdividing the range of economic objective function into 8 equidistant points. Each point on the
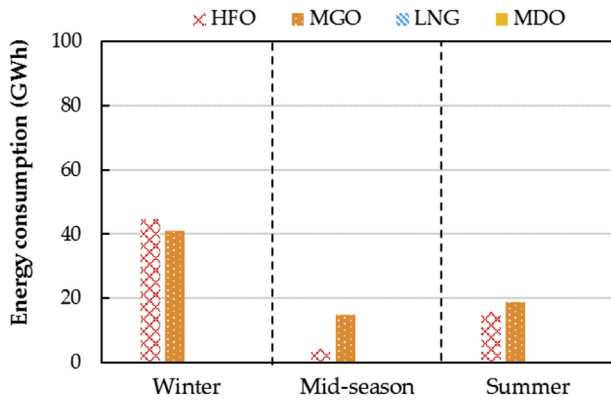
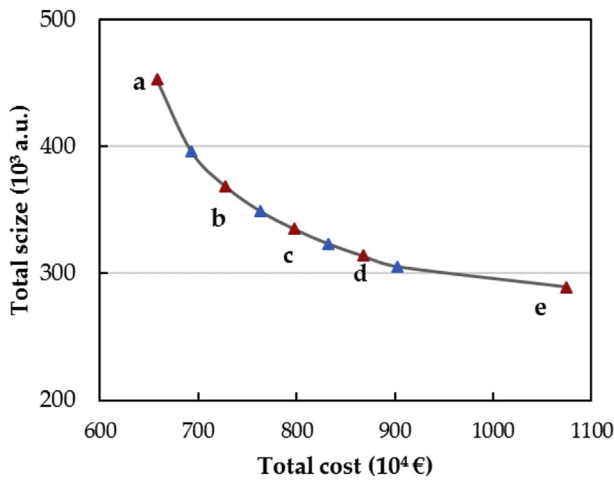**Fig. 15.** Energy consumption of the cruise ship's energy system under case 3.

Fig. 16. Pareto frontier obtained under the economic and size objectives.

Table 4
Optimized energy system configurations and energy consumption at points b, c, and d on the Pareto Frontier.

Facility	Point b	Point c	Point d
PV panels (m^2)	-	-	-
Wind turbine (m^2)	-	-	-
Compression chiller (kW)	1,400	1,400	1,400
Internal combustion engine (kW)	6,686	5,552	5,322
Gas turbine (kW)	8,010	10,331	11,671
Dual fuel engine (kW)	6,557	4,636	2,984
Exhaust gas boiler (kW)	7,260	7,260	7,260
Selective catalytic reactor (kW)	1,233	1,233	1,476
Exhaust scrubbers (kW)	987	987	1,181
Batteries (kWh)	5,000	4,626	4,611
HFO consumption (GWh)	47.82	51.12	58.85
MGO consumption (GWh)	16.20	29.52	39.92
LNG consumption (GWh)	77.33	58.00	38.22
MDO consumption (GWh)	-	-	-
Total annual cost (10^4 €)	728.17	798.17	868.17
Total weight (ton)	356.25	324.17	304.44
Total volume (m^3)	12,046.08	10,392.10	8,995.36
Total size (10^3)	368.30	334.57	313.44

large size. However, under the size objective optimization, due to the large size of the dual fuel engine and its fuel LNG, it is eliminated and replaced by internal combustion engine to provide energy to cruise ship, resulting in the increase in the capacity of internal combustion engine. Furthermore, as expected, the capacity of battery decreases with the increase of the size objective ratio.

4.2.5. Comprehensive analysis

In order to compare the results of single-objective and multi-objective optimization, Fig. 17 shows the total annual cost and size at points a, b, c, d, and e on the Pareto frontier. The trend of the total annual cost of the optimized energy system is opposite to the size from point a to point e. With the increase of the size objective ratio, the total cost increases and the size decreases gradually. The ratios of total annual cost and size reduction are also calculated and presented in Fig. 17. Point e has the highest size reducing ratio, 21.1%. However, the cost saving ratio is −42.7%. This is because the economic objective is ignored, and only the size objective is taken into account. In such a context, the large-size facility or facility that requires large-size energy carrier should not be selected as much as possible, and the configuration of energy system at point e is not cost-effective.

Furthermore, the pollutant emissions are given in Fig. 18, it can

Pareto frontier represents an optimized configuration of the cruise ship's energy system, thereby providing different options for ship designers. It can be found that the range of total annual cost is between 6,851,777 € and 10,747,140 € and the range of size is between 289,124 and 452,774.

For convenience, points b, c, and d are selected, and these three points are considered sufficient to describe the combination of economic and size objectives. Table 4 shows the optimized energy system configurations and energy consumption at points b, c, and d on the Pareto frontier. Not surprisingly, PV panels and wind turbines are not selected in any configuration because the solar radiation and wind power are insufficient, and the capacity of compression chiller is the same as 1400 kWh. The capacity of gas turbine increases with the increase of the size objective ratio, along with the increase in the energy consumption of MGO. This result clearly shows that gas turbines and MGO are more in line with the requirement of the size objective. On the contrary, the capacity of dual fuel engine decreases with the increase of the size objective ratio, due to the high linear capacity-dependent volume and weight, accompanied by a reduction in LNG consumption. The trend of the internal combustion engine's capacity is complicated, at first it reaches the maximum of 13,884 kW under the economic objective, and decreases with the increase of the size objective ratio, whereas it increases under the size objective (at point e). This phenomenon can be explained by the following reasons: with the increase of the size objective ratio, the capacity of the internal combustion engine decrease (at points a, b, c and d) because of its
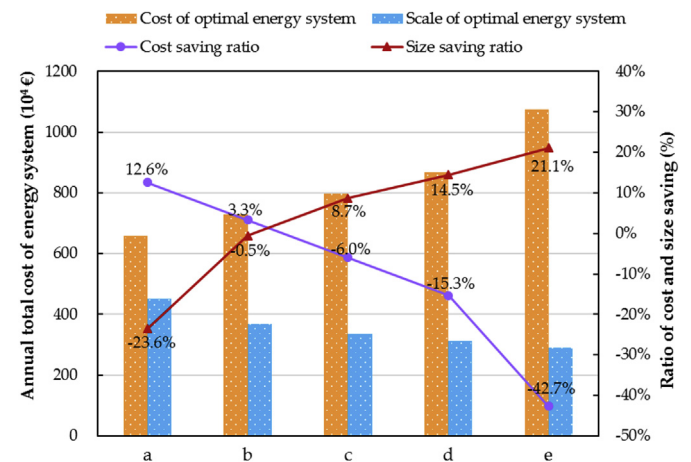

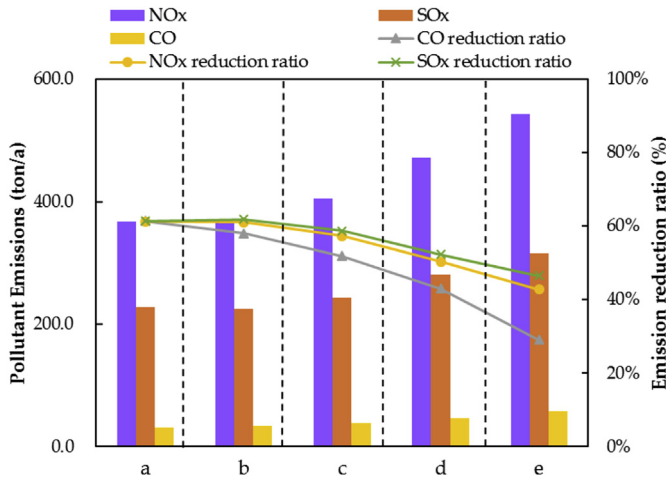**Fig. 17.** Total annual cost and size at points a, b, c, d and e on the Pareto Frontier.

Fig. 18. Pollutants emissions at points a, b, c, d and e on the Pareto Frontier.

$$f_{per}^{scale} = \frac{10000 \times \left(f_{scale}^{RES} - f_{scale}^{OER}\right)}{f_{\cos t}^{OER}} \quad (35)$$

$$f_{per}^{emission} = \frac{10000 \times \left(f_{emission}^{RES} - f_{emission}^{OER}\right)}{f_{\cos t}^{OER}} \quad (36)$$

be concluded that the optimal system can reduce the annual CO emissions by 29.1%–61.3%, reduce the annual NOx emissions by 42.8%–61.3%, and reduce the annual SOx emissions by 46.5%–61.4%. Compared to the reference energy system, the reduced sizes and pollutant emissions (kg) per 10,000 € in optimal energy system are calculated according to Eq. (35) and Eq. (36), and the calculted results are presented in Table 5. It can be noted that point a has the highest pollutant emission reduction, which means that compared with the reference energy system, using 10,000 € could reduce 75.3 kg CO emissions, 855.0 kg NOx emissions and 550.1 kg SOx emissions under economic objective. However, point a causes an increase in size, further illustrating that only considering the economic objective will lead to poor cost performance. As can be seen from Table 5, with the increase of the size objective ratio (at points c, d, and e), the pollutant emissions and sizes reduction become positive, which means that the great cost performance occurred. Therefore, it is unreasonable to design cruise energy system only considering economy. Factors such as size and pollutant emissions should also be considered. Moreover, the larger the size objective ratio is, the more size is saved, but the more the pollutant emissions are.

Fig. 19 gives the total annual energy consumption and the ratio of fuel consumption to the total. It can be noted that the total annual energy consumption first decreases at points a, b, c and d, then increases at point e. With the increase of the size objective

Table 5
Cost performance at points a, b, c, d and e on the Pareto Frontier.

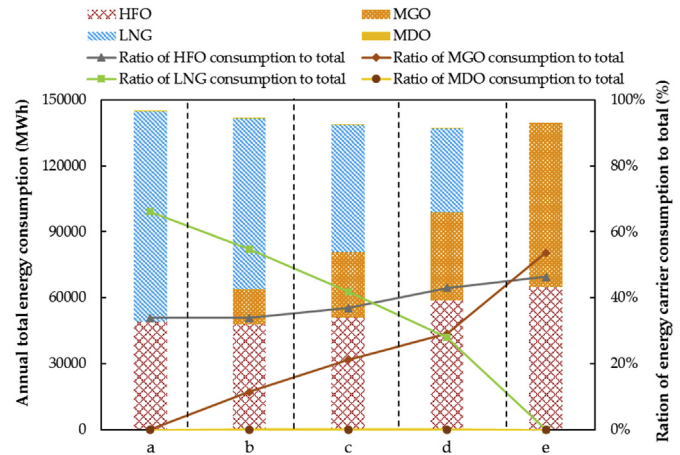| Cost performance	Point a	Point b	Point c	Point d	Point e
Total annual cost (10^4 €)	658.17	728.17	798.17	868.17	1074.71
CO reduction (kg/10^4 €)	75.3	64.4	52.6	40.1	21.9
NOx reduction (kg/10^4 €)	885.0	796.4	682.5	551.5	378.9
SOx reduction (kg/10^4 €)	550.1	500.8	434.3	355.7	255.4
Size reduction (-/10^4 €)	−131.4	−2.7	39.8	60.9	71.8

Fig. 19. Energy consumption and the ratio of energy carrier consumption to total at points a, b, c, d and e on the Pareto Frontier.

ratio, the ratio of LNG consumption sharply decreases, while the ratio of MGO consumption significantly increases, particularly from point d to point e. This is because that LNG has a large value of size, and MGO has a small value of size. The reduction in size comes mainly from the reduction of natural gas consumption and the increase of MGO consumption.

Fig. 20 shows the components of the total annual cost and size at points a, b, c, d and e on the Pareto Frontier. It is worth noting that MDO is not selected in any configuration and therefore its cost and size are not presented. For Fig. 20(a), the cost is composed of the facilities cost and three fuels consumption cost. Similarly, the size consists of the size of facilities and three fuels as shown in Fig. 20(b). In order to study the changing trends in each of the cost and size component, the cost and size are standardized. For instance, the yellow solid line represents the LNG consumption cost, and the sum of five points on this line is equal to 1. With the increase of the size objective ratio, the cost of MGO and LNG consumption changes significantly. On the contrary, there is no obvious change in the cost of facilities and HFO consumption, because point e only considers the size objective. Therefore, LNG and MDO are not selected as the primary energy, and gas turbines and MGO are selected as the energy provider. The same phenomenon occurs in the component of size. As can be seen from Fig. 20(b), the size of MGO and LNG changes significantly with the increase of the size objective ratio. Based on the analysis above, the size and consumption cost of MGO and LNG are more sensitive to the change of the size objective ratio.

5. Conclusions

For the first time, this paper studied the size in design optimization of cruise ship's energy system. Based on the pre-established cruise ship's structure with multiple facilities, a multi-objective mathematical programming model is formulated to determine the type, capacity of facilities and operation strategies with minimal total annual cost and size. The MOMP problem is solved by the augmented ε-constraint method and the Pareto frontier obtained can provide ship designers with a good balanced solutions for the economic and size objectives. Finally, the model is applied to a cruise ship operating in the Baltic Sea between Stockholm on the Swedish mainland and Mariehamn on the Åland islands. According to the results, the following conclusions can be drawn:

(1) In the single economic optimization, the optimal energy system has a better economic performance than the reference
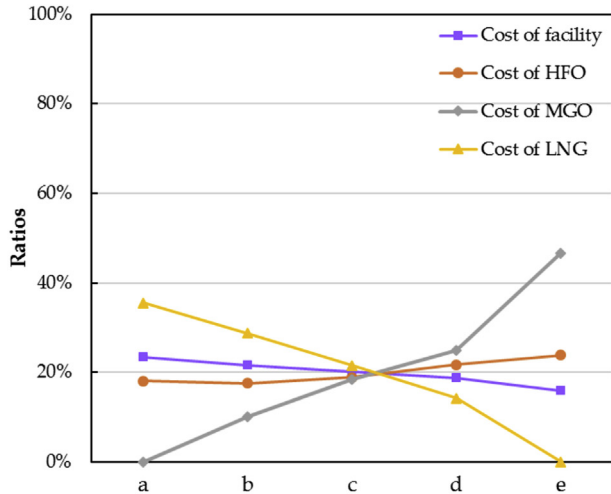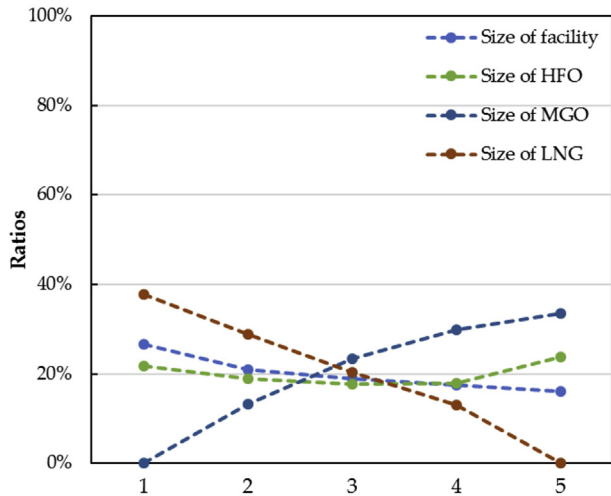
Fig. 20. The components of (a) total annual cost and (b) size at points a, b, c, d and e on the Pareto Frontier.

energy system with a 9.8% reduction in the total annual cost. When considering both the economic and size objectives, the optimal system can reduce the CO emissions by 29.1%–61.3% per year, reduce the NOx emissions by 42.8%–61.3% per year, and reduce the SOx emissions by 46.5%–61.4% per year.

(2) In the multi-objective optimization, the design and operation strategies as well as size of energy system for cruise ships could be obtained with minimal total annual cost and size. With the increase of the size objective ratio, the total annual cost increases and the size decreases gradually. However, the cost-saving ratio is negative compared to the reference energy system when only considering the size objective. On the contrary, the size-reducing ratio is negative if only the economic objective is taken into account.

(3) A sensitivity analysis is conducted to explore the impact of the change of size objective ratio on the size and cost of energy fuels. The results show that compared with HFO and MDO, the size and consumption cost of MGO and LNG are more sensitive to the change of size objective ratio.

This paper can be an initiative of the economical and size evaluation of the different technologies for the ship owners, considering fuel costs, emission reduction requirements and profitable size availability. Moreover, it can help ship owners to design the energy system to comply with the emission regulations. Nevertheless, further studies are still required for a more comprehensive conclusion, such as the reliability and flexibility assessments of energy system supply. Meanwhile, future work could study the impact of different carbon emission limits on the cruise ship's energy system structure and investment costs.

Acknowledgements

Nomenclature

Sets and indices

$i \in I$	All facilities: PV, WT, COC, ICE, GT, DF, EGB, SCR, ES, BT
$j \in J$	Energy allocation facilities: PV, WT, COC, ICE, GT, DF, EGB, SCR, ES
$m \in M$	Energy carriers: HFO, MGO, LNG, MDO
$s \in S$	Number of operation status
$ts \in TS_s$	Number of time steps of operation status s
$ts \in \overline{TS_s}$	Number of time steps of the first operation status

Continuous Parameters

CRF_i	Capital recovery factor of facility i [-]
C_{FCi}	Fixed cost of installing facility i [€]
C_{LCi}	Linear capacity-dependent cost of installing facility i [€/kW, €/kWh, €/m2]
$C_{s,m}$	Carbon emissions factor of energy carrier m for operation state s [g CO2/kWh]
Carbon$_s$	Upper limit of carbon emissions for operation state s [g CO2]
$CD_{s,ts}$	Cooling demand of cruise ship at time step ts for operation state S [kWh]
$ED_{s,ts}$	Electricity demand of cruise ship at time step ts for operation state s [kWh]
f_{per}^{scale}	The reduction sizes with regard to the reference energy system using the unit money [-/€]
f_{scale}^{RES}	The total size of the reference energy system [-]
f_{scale}^{OER}	The total size of the optimal energy system [-]
$f_{cos,t}^{OER}$	The total annual cost of the optimal energy system [€]
$f_{per}^{emission}$	The reduction pollutant emissions with regard to the reference energy system using the unit money [kg/€]
$f_{emission}^{RES}$	The total pollutant emissions of the reference energy system [kg]
$f_{emission}^{OER}$	The total pollutant emissions of the optimal energy system [kg]
$IN_{s,ts}^{PV}$	Incoming solar radiation at time step ts for operation state s [kWh/m2]
$IN_{s,ts}^{WT}$	Incoming wind power at time step ts for operation state s [kWh/m2]
$lifetime_i$	Lifetime of facility i [years]
Max	The upper limit to the capacity of facilities [kW, kWh, m2]
Min	The lower limit to the capacity of facilities [kW, kWh, m2]

$MD_{s,ts}$	Mechanical demand of cruise ship at time step *ts* for operation state *s* [kWh]
$N_{s,m}$	NOx emission factor of energy carrier *m* for operation state *s* [g NOx/kWh]
$Nitrogen_s$	Upper limit of NOx emission for operation state *s* [g NOx]
n_i	Conversion efficiency of facility *i* [-]
n_{ch}	Charging efficiency of battery [-]
n_{dis}	Discharging efficiency of battery [-]
n_{loss}	Self-discharge losses of battery [-]
P_m	Price of energy carrier *m* [€/kWh]
r	Discount rate [-]
S_{LSi}	Linear capacity-dependent occupy space of installing facility *i* [m3/kW, m3/kWh]
S_{LOm}	Linear-consumption occupy space of energy carrier *m*. [m3/kWh]
S_{max}^{PV}	Maximum area for installation of PV panels [m2]
S_{max}^{WT}	Maximum area for installation of wind turbines [m2]
$Su_{s,m}$	SOx emission factor of energy carrier *m* for operation state *s* [kg SOx/kWh]
$Sulfur_s$	Upper limit of SOx emission for operation state *s* [kg SOx]
$TD_{s,ts}$	Thermal demand of cruise ship at time step *ts* for operation state *s* [kWh]
$w_{s,ts}$	Total number of time step *ts* for operation state *s* [-]
W_{LSi}	Linear capacity-dependent weight of installing facility *i* [kg/kW, kg/kWh]
W_{LOm}	Linear-consumption weight of energy carrier *m*. [kg/kWh]
α	Scaling factor [-]
λ	Conversion factor [kg/m2]
β	Conversion factor [kg/m2]
ε	Height of PV panels [m]
ϕ	Height of wind turbine [m]

Positive continuous variables

$EX_{s,ts,m}$	Consumption of energy carrier *m* at time step *ts* for operation state *s* [kWh]
$ES_{s,ts}^{ch}$	Charging rate of battery at time step *ts* for operation state *s* [kWh]
$ES_{s,ts}^{dis}$	Discharging rate of battery at time step *ts* for operation state *s* [kWh]
$Q_{s,ts,i}$	Energy input to the facility *i* at time step *ts* for operation state *s* [kWh]
$S_{s,ts}$	Energy stored in battery at time step *ts* for operation state *s* [kWh]
V_i	Capacity of facility *i* [kW for conversion facilities, kWh for battery, m2 for PV panels and wind turbines]

Binary variables

B_i	If the facility *i* is selected to install in the cruise ship, $B_i = 1$. Otherwise, $B_i = 0$

Acronyms

RES	Reference energy system
OES	Optimal energy system
ICE	Internal combustion engine
DF	Dual fuel engine
EGB	Exhaust gas boiler
GT	Gas turbine
SCR	Selective Catalytic Reactor
ES	Exhaust scrubber
COC	Compression chiller
PV	PV panels
WT	Wind turbine
HFO	Heavy fuel oil

MGO	Marine gas oil
LNG	Liquefied natural gas
MDO	Marine diesel oil
PM	Prime Movers
CO	Carbon Oxide
CO2	Carbon Dioxide
NOx	Nitrogen Oxides
SOx	Sulphur Oxides
MILP	Mixed-integer linear programming
MINLP	Mixed integer nonlinear programming
MOMP	Multi-objective mathematical programming

References

Ancona, M.A., Baldi, F., Bianchi, M., Branchini, L., Melino, F., Peretto, A., Rosati, J., 2018. Efficiency improvement on a cruise ship: load allocation optimization. Energy Convers. Manag. 164, 42—58.

Armellini, A., Daniotti, S., Pinamonti, P., Reini, M., 2018. Evaluation of gas turbines as alternative energy production systems for a large cruise ship to meet new maritime regulations. Appl. Energy 211, 306—317.

Bicer, Y., Dincer, I., 2018a. Clean fuel options with hydrogen for sea transportation: a life cycle approach. Int. J. Hydrogen Energy 43 (2), 1179—1193.

Bicer, Y., Dincer, I., 2018b. Environmental impact categories of hydrogen and ammonia driven transoceanic maritime vehicles: a comparative evaluation. Int. J. Hydrogen Energy 43 (9), 4583—4596.

Burel, F., Taccani, R., Zuliani, N., 2013. Improving sustainability of maritime transport through utilization of Liquefied Natural Gas (LNG) for propulsion. Energy 57, 412—420.

Chen, J., Wang, F., Stelson, K.A., 2018. A mathematical approach to minimizing the cost of energy for large utility wind turbines. Appl. Energy 228, 1413—1422.

CLIA, 2016. 2016 Cruise Industry Outlook. Cruise Lines International Association, Florida, 2016.

Di Somma, M., Yan, B., Bianco, N., Graditi, G., Luh, P.B., Mongibello, L., Naso, V., 2017. Multi-objective design optimization of distributed energy systems through cost and exergy assessments. Appl. Energy 204, 1299—1316.

Esmaili, M., Amjady, N., Shayanfar, H.A., 2011. Multi-objective congestion management by modified augmented ε-constraint method. Appl. Energy 88 (3), 755—766.

Finnish Meteorological Institute. Available at. https://en.ilmatieteenlaitos.fi/marine-weather-and-baltic-sea. accessed on 10.15.2018.

Grabowski, M., Hendrick, H., 1993. How low can we go?: validation and verification of a decision support system for safe shipboard manning. IEEE Trans. Eng. Manag. 40 (1), 41—53.

Hu, Q.-M., Hu, Z.-H., Du, Y., 2014. Berth and quay-crane allocation problem considering fuel consumption and emissions from vessels. Comput. Ind. Eng. 70, 1—10.

Li, L., Mu, H., Li, N., Li, M., 2016. Economic and environmental optimization for distributed energy resource systems coupled with district energy networks. Energy 109, 947—960.

Livanos, G.A., Theotokatos, G., Pagonis, D.-N., 2014. Techno-economic investigation of alternative propulsion plants for Ferries and RoRo ships. Energy Convers. Manag. 79, 640—651.

Mavromatidis, G., Orehounig, K., Carmeliet, J., 2018. Design of distributed energy systems under uncertainty: a two-stage stochastic programming approach. Appl. Energy 222, 932—950.

Mavrotas, G., 2009. Effective implementation of the ε-constraint method in multi-objective mathematical programming problems. Appl. Math. Comput. 213 (2), 455—465.

Mondejar, M.E., Ahlgren, F., Thern, M., Genrup, M., 2015. Study of the on-route operation of a waste heat recovery system in a passenger vessel. Energy Procedia 75, 1646—1653.

Motley, M.R., Nelson, M., Young, Y.L., 2012. Integrated probabilistic design of marine propulsors to minimize lifetime fuel consumption. Ocean Eng. 45, 1—8.

Nguyen, P., Tenno, R., 2016. Waste-heat recovery estimation on ships by means of conditionally-gaussian filtering. IFAC-PapersOnLine 49 (23), 408—413.

Nielsen, K.V., Blanke, M., Eriksson, L., Vejlgaard-Laursen, M., 2018. Marine diesel engine control to meet emission requirements and maintain maneuverability. Contr. Eng. Pract. 76, 12—21.

Perry Hobson, J.S., 1993. Analysis of the US cruise line industry. Tourism Manag. 14 (6), 453—462.

Rodríguez-Rodríguez, D., Malak, D.A., Soukissian, T., Sánchez-Espinosa, A., 2016. Achieving Blue Growth through maritime spatial planning: offshore wind energy optimization and biodiversity conservation in Spain. Mar. Policy 73, 8—14.

Song, D.-P., Xu, J., 2012. An operational activity-based method to estimate CO2 emissions from container shipping considering empty container repositioning. Transport. Res. Transport Environ. 17 (1), 91—96.

Stefanidaki, E., Lekakou, M., 2014. Cruise carrying capacity: a conceptual approach. Res. Transport. Bus. Manag. 13, 43—52.

Tang, R., Li, X., Lai, J., 2018a. A novel optimal energy-management strategy for a maritime hybrid energy system based on large-scale global optimization. Appl.

Energy 228, 254–264.

Tang, R., Wu, Z., Li, X., 2018b. Optimal operation of photovoltaic/battery/diesel/cold-ironing hybrid energy system for maritime application. Energy 162, 697–714.

Trivyza, N.L., Rentizelas, A., Theotokatos, G., 2018. A novel multi-objective decision support method for ship energy systems synthesis to enhance sustainability. Energy Convers. Manag. 168, 128–149.

Xie, G., 2011. Optimal preliminary propeller design based on multi-objective optimization approach. Procedia Eng. 16, 278–283.

Xing, X., Yan, Y., Zhang, H., Long, Y., Wang, Y., Liang, Y., 2019. Optimal design of distributed energy systems for industrial parks under gas shortage based on augmented ε-constraint method. J. Clean. Prod. 218, 782–795.

Yang, Y., Zhang, S., Xiao, Y., 2017. Optimal design of distributed energy resource systems based on two-stage stochastic programming. Appl. Therm. Eng. 110, 1358–1370.